International Journal of Technology v(i) pp-pp (YYYY)
Received Month Year / Revised Month Year / Accepted Month Year

International Journal of Technology

http://ijtech.eng.ui.ac.id

A Robust SQP Optimization Technique for PID Controller of Boost Converter in BLDC Motor Considering Renewable Energy Sources

Abstract. The development of renewable energy has had a positive impact on reducing the level of emissions produced by fossil fuels. One of the renewable energies that currently has a fairly high level of efficiency is Photovoltaic. Motors supplied with Photovoltaic have a low starting voltage and cause voltage fluctuations so that the stability and performance of the motor are reduced. One method that can be used to reduce voltage fluctuations is to control its stability. This can be done by adding a boost converter that is optimized using PID. Several methods that are often used to find the right value include the trial and error method and the numerical optimization method. This paper discusses the optimization of PID tuning on boost converters and BLDC motors using the Sequential Quadratic Programming (SQP) method. Tuning using SQP that has been carried out provides an overshoot value of 0%, and a completion time of 480 s, much smaller than metaheuristic-based ones such as GMO 379 s and FA 1108 s. In addition, the simulation time obtained on SQP is 13.25 times faster than GMO and 16.41 times faster than FA. Considering the performance in terms of the Integral of Time-weighted Absolute Error (ITAE), SQP has a better performance by 1018555 compared to the metaheuristic method which has a performance of 1097300. This difference indicates that SQP produces a more optimal ITAE value by 7.18% compared to FA and 9.64% compared to GMO, which is a metaheuristic method.

Keywords: Robust SQP optimization; PID controller; Boost converter; BLDC motor; Renewable energy

1. Introduction

The global shift towards renewable energy sources has been instrumental in mitigating the environmental impact of fossil fuel emissions. Among these renewable energy technologies, photovoltaic (PV) systems have emerged as a highly efficient solution. Solar PV technology harnesses sunlight and converts it directly into electricity through the photovoltaic effect, making it a clean and sustainable energy source (Aiman Setiawan, 2017; Ajiwiguna and Kirom, 2024; Ali et al., 2024; Saaid et al., 2018). However, integrating PV systems with motors poses challenges due to their low starting voltage and inherent voltage fluctuations, leading to compromised stability and performance. To address these challenges, various methods have been explored, with one promising approach being the integration of boost converters optimized through proportional-integral-derivative (PID) control (Ben Safia et al., 2021; Malla et al., 2022; Mohammed and Farah, 2019; Munisekhar et al., 2020). Traditional tuning methods for PID controllers, such as trial and error and numerical optimization, have been widely employed but are often time-consuming and inefficient.

The global shift towards renewable energy sources has become an important cornerstone in efforts to reduce the negative impact that fossil fuel emissions have on the environment.

In this context, renewable energy technologies, especially photovoltaic (PV) systems, have emerged as a highly efficient and promising solution (Jia et al., 2019; Kumar and Vinaykumar, 2023; Setyawati et al., 2024). However, the challenges that arise in integrating a PV system with a motor are a major concern, especially due to the presence of low starting voltages and naturally occurring voltage fluctuations, which directly impact the stability and performance of the entire system (Anshory et al., 2024; De et al., 2020; Osman et al., 2022). To overcome this complexity, various strategies and methods have been studied, and among them, a promising approach is the integration of optimized boost converters via proportional-integral-derivative (PID) control (Aguila-Leon et al., 2021; Devaraj et al., 2021; Khleaf et al., 2019).

PID is a type of controller primarily used for error correction. For controlling voltage in a system, it addresses voltage deviations occurring between the system output and the PID controller input. Compared to other control methods, such as Fuzzy Logic, Artificial Neural Networks (ANN), and similar approaches, PID is relatively simple. It only requires three parameters—Proportional, Integral, and Derivative—to deliver effective results. These parameters can initially be set manually using random values or through trial-and-error. However, traditional methods for tuning PID parameters, such as trial-and-error methods and numerical optimization, although frequently used, are often faced with time and efficiency constraints (Aseem and Selva Kumar, 2020). To achieve optimal performance, an optimization process is necessary, as better optimization algorithms yield better results. Despite its simplicity, PID can correct system errors effectively, offering robust performance that can be evaluated through parameters such as undershoot, overshoot, rise time, and the speed to reach steady state (Hekimoğlu and Ekinci, 2020).

Other control method, such as fuzzy logic, can also achieve good results, however, they often require numerous rules to ensure optimal performance. Developing these rules involves significant manipulation and adjustment. The construction of a fuzzy logic rule-based is a computationally intensive task that requires considerable effort to attain an accurate and efficient set of rules (Izci et al., 2022; Ghamari et al., 2022). Similarly, another method for instance ANN is versatile and applicable to various systems, but it requires extensive data for the training process, which can be time-intensive (Khleaf et al., 2019; Devaraj et al., 2021). Furthermore, determining the optimal number of hidden layers and neurons necessitates additional optimization. Given the lengthy training time for ANN models, this method may not be suitable for applications requiring immediate results. Hence, for applications demanding timely solutions, PID controllers, particularly when their parameters are fine-tuned, still outperform other control strategies.

Therefore, this research aims to examine a new approach using a derivative-based optimization technique, Sequential Quadratic Programming (SQP) in optimizing PID parameters in converters integrated with BLDC motors, with the hope of overcoming these challenges more effectively and efficiently. Several derivative-based methods, such as quadratic programming and linear programming, offer rapid computation times for finding optimal parameters (Delfianti et al., 2022; Sugiantoro et al., 2021; Wibowo et al., 2023). However, these methods are limited to problems where the objective function is either quadratic or linear.

The parameterization of solar PV systems is crucial for accurately modeling their behavior and integrating them into the boost converter-BLDC motor system. Parameters such as solar irradiance, temperature, panel orientation, and efficiency are meticulously considered in the research to capture the dynamic nature of solar energy generation (Bueso et al., 2022; Eleftheratos et al., 2024; Liu et al., 2022; Osorio et al., 2019). By incorporating these parameters into the modeling framework, the research aims to simulate real-world conditions and evaluate the performance of the proposed robust SQP optimization technique for PID controller design. This comprehensive approach enables a thorough analysis of the system's response to varying solar conditions, ultimately facilitating the development of efficient and reliable renewable energy systems for practical applications. Based on previous research conducted by (Anshory et al., 2024).

In addition to the technical challenges faced in integrating a photovoltaic (PV) system with a motor, the economic aspect is also an important consideration. Although PV technology offers an environmentally friendly and efficient solution, high initial investment costs are often a barrier for many system owners. Therefore, developing methods that can improve the efficiency and performance of PV-motor systems without sacrificing stability or requiring large additional investments is essential. In this context, optimization of PID parameters using the SQP method can be a promising solution, because it can produce more optimal tuning with lower computational costs, which ultimately can reduce the total system operational costs (Khodabakhshian et al., 2012).

The role of the boost converter system is also worth noting in this context. The boost converter plays a key role in regulating the output voltage of the PV panel to ensure the smooth operation of the motor. However, voltage fluctuations that occur can affect overall system stability, especially in the case of motors that require a stable starting voltage to start operation (Alshareef et al., 2021; Hamid et al., 2021; Miqoi et al., 2019). Therefore, optimization of the amplifier converter simultaneously with PID tuning becomes important to achieve an optimal balance between system stability and performance (Ghamari et al., 2022; Hekimoğlu and Ekinci, 2020; Izci et al., 2022; Mitra and Rout, 2022). PID control is needed to stabilize the system, improve response, and reduce errors and flexibility to obtain optimal performance.

In evaluating the effectiveness of the SQP method in optimizing PID parameters, comparisons with alternative methods also need to be carried out. Genetics-based metaheuristics or differential evolutionary algorithms may offer different approaches in the search for optimal parameters (Gao, 2023; Janprom et al., 2020; Joseph et al., 2022). Therefore, comparative analysis between SQP methods and alternative methods such as genetics, differential evolution, or genetic algorithms can provide deeper insight into the advantages and disadvantages of each approach. Evaluation should not only focus on system performance under simulated conditions, but also need to carry out practical testing in the field. Practical testing will provide a better understanding of the effectiveness of PID tuning optimized using the SQP method in real operational conditions. The results of these field tests can be a valuable guide for practical applications in industry and society. In discussing research results, it is important to identify the limitations and weaknesses of the proposed approach. Acknowledging limitations and weaknesses can open the door to continued research and further development, as well as provide direction for future research in an effort to overcome remaining challenges in PV-motor system integration.

The integration of BLDC motors with photovoltaic systems has emerged as a promising approach in the field of renewable energy and efficient power conversion. Photovoltaic systems, which generate electricity from solar energy, can be effectively combined with BLDC motors to power a variety of applications, particularly in the context of water pumping and other sustainable energy solutions. One of them is the application of BLDC in air conditioning systems (Nasruddin and Sinambela, 2015).In addition, the implementation of this system is applied to a water pump system powered by solar energy. This pump is used for the agricultural sector, it can also be used in urban areas.

This paper focuses on the optimization of PID tuning for boost converters and brushless DC (BLDC) motors using the Sequential Quadratic Programming (SQP) method. SQP offers a computationally efficient alternative to traditional optimization techniques, promising significant reductions in simulation time (Grigoraș et al., 2022; Luo et al., 2022; Mao et al., 2019; Mohasseb et al., 2017). This research provides a contribution regarding the use of the Sequential Quadratic Programming (SQP) method to optimize PID parameters in DC-DC converters integrated with brushless DC (BLDC) motor. This approach offers an innovative solution to improve the stability and performance of PV-motor systems, with a focus on better computing time efficiency than traditional methods. In addition, the development of methods that can provide more optimal PID tuning with lower computational costs, thereby overcoming the time and efficiency constraints often faced by traditional methods. In terms of urgency, this research provides a perspective regarding the need to overcome the challenges of PV-motor system integration in an effective and efficient manner, in order to increase the adoption of renewable energy technologies and reduce dependence on fossil energy sources that are detrimental to the environment. Thus, this research not only makes a significant contribution to the development of renewable energy technology, but also has a positive impact on efforts to mitigate global climate change.

2. Methods

In this research, solar photovoltaic (PV) systems play a pivotal role in providing renewable energy input to the overall system. Based on previous research conducted by (Anshory et al., 2024). Therefore, this research uses fundamental Eq. (1) and (2) which assume a relationship between basic current interactions and factors that determine solar cell performance.

$$I = I_{Ph} - I_d - I_p \tag{1}$$

$$I = I_{Ph} - I_0 \left\{ e^{\frac{q(V+R_S I)}{AKT}} - 1 \right\} - \frac{V+R_S I}{R_p} \tag{2}$$

In this context, I represents the total photovoltaic output current, I_{ph} denotes the photocurrent, and I_d refers to the diode current, which can be expressed as Eq. (3)

$$I_d = I_0 \left\{ e^{\frac{q(V+R_S I)}{AKT}} - 1 \right\} \tag{3}$$

Here, I_0 indicates the diode reverse saturation current, I_p is the parallel current, R_p represents the parallel resistance, R_S denotes the series resistance, and q is the electron charge (1.6 10^{-19}C). The variable V represents the open circuit output voltage across the photovoltaic cell, while K stands for the Boltzmann constant. In a short circuit condition, where I_{ph} can be substituted with the short circuit current I_{SC}, R_p is considered infinite, and the third term in the preceding equation is omitted. Equation (4) provides a clear explanation of the analysis and optimization of solar cell performance concerning current and voltage variations under different operational conditions.

$$I = I_{SC} - I_0 \left\{ e^{\frac{q(V+R_S I)}{AKT}} - 1 \right\} \tag{4}$$

The output of PVs depends on several factors of weather and environment, especially the ambient temperature and solar radiation. It is the expression that allows describing the relation between the voltage across a photovoltaic cell with its internal elements, also contemplating the most relevant factors of the diode voltage, current, and series resistance; see Eq. (5).

$$V_{PV} = V_d - I_{PV} R_s \tag{5}$$

The parameters of the 200 Wp solar panel Grape Solar GS-P-200-CSPE used in this study are detailed in Table 1 (MathWorks, 2004).

Table 1. Electrical parameters of the 200 W photovoltaic panel

Parameters	Value
Maximum power (W)	200.277
Cells per module (Ncell)	60
Open circuit voltage Voc (V)	36.2
Short-circuit current Isc (A)	7.68
Voltage at maximum power point Vmp (V)	28.9
Current at maximum power point Imp (A)	6.93
Temperature coefficient of Voc (%deg.C)	-0.37
Temperature coefficient of Isc (%deg.C)	0.13

2.1. Boost Converter and BLDC Motor

The boost converter system is a key component in the integration of photovoltaic (PV) systems with brushless DC (BLDC) motors. The boost converter is tasked with changing the output voltage produced by the PV panel into a voltage suitable for driving the BLDC motor with optimal efficiency. In general, an amplifier converter works by increasing a low input voltage to a higher output voltage. In this context, the description of the amplifier converter system will include technical specifications such as input and output voltages, maximum current, conversion efficiency and integrated safety features. Meanwhile, brushless DC (BLDC) motors are a type of electric motor that is increasingly popular because of its efficiency, reliability and good control. BLDC motors do not have friction brushes like conventional DC motors, which makes them more durable and requires less maintenance. A description of a BLDC motor will include its physical and electrical characteristics, such as the number of phases, maximum torque, maximum rotational speed, and control configuration used. In addition, the system description will also cover the interaction between the boost converter and the BLDC motor, including how the output voltage of the boost converter is controlled and adjusted to match the operational requirements of the BLDC motor. This includes an explanation of how PID control is integrated with the system to ensure voltage stability and optimal motor performance. Thus, this system description will provide a comprehensive understanding of how boost converters and BLDC motors interact in PV-motor integration applications, as well as how PID control is used to optimize overall system performance.

2.2. SQP Optimization

The SQP method is an optimization technique used to solve nonlinear optimization problems with nonlinear constraints.

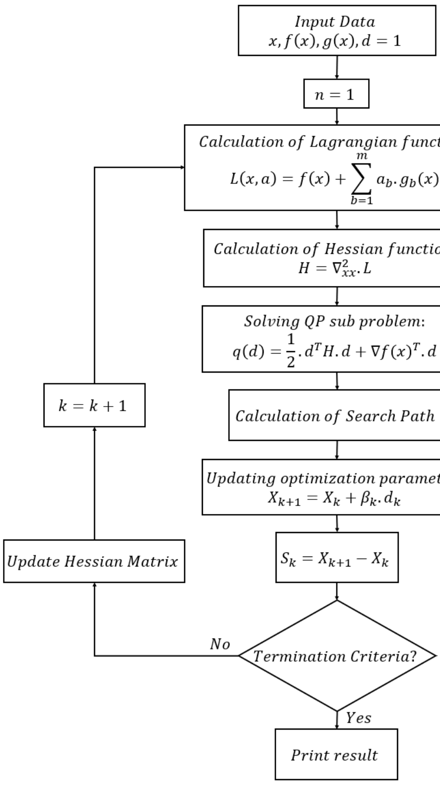

Figure 1 The flowchart of the SQP method

The basic principle of SQP involves iteration to improve the solution gradually until it reaches convergence to the optimal solution. In the initial stage, SQP starts by guessing the starting point and updating the point through iterative steps. Each iteration involves the following steps: first, defining a quadratic model of the original optimization problem around the point being evaluated; second, solve the resulting sub quadratic problem to generate search directions; and third, perform a search step in the given direction to update the points and continue the iteration. This process is repeated until the convergence criteria are met or an optimal solution is found.

In the context of this research, SQP is applied to solve optimization problems involving tuning PID parameters in amplifier converters and PID control in BLDC motors. Therefore, this section will also discuss how the optimization problem is structured to take into account the optimization objectives, constraints, and decision variables involved. SQP is then applied to solve this problem by considering the mathematical structure of the problem and using iterative techniques to reach an optimal solution. Thus, the explanation of the basic principles and implementation of SQP in this research will provide a deep understanding of how this optimization method is applied to overcome challenges in PV-motor system integration.

Figure. 1 proposes the general flowchart of the SQP method. The algorithm can be summarized as follows:

$\min f\ (x)$

Subject to: $g_b(x) \leq 0, b = 1, \ldots, m$

where *x* shows the PID controller parameters that should be optimized, *f(x)* is the objective function given in Eq. (6) and *g(x)* is the inequality constraint. This algorithm proposed in this paper as follows (Khodabakhshian et al., 2012):

At iteration *k* = 1,

Step 1: The Lagrangian of this problem is defined as:

$$L(x, \alpha) = f(x) + \sum_{b=1}^{m} \alpha_b g_b\,(x) \tag{6}$$

where α is the vector of approximate Lagrange multipliers. With x_n as the PID controller gains in the current iteration and the current approximate Hessian (H_n). The Quadratic programming (QP) is defined as:

$$\min q(d) = \frac{1}{2} d^T H d + \nabla f(x)^T d \tag{7}$$

where d is the current iteration for search direction. The matrix H is a positive definite approximation of the Hessian matrix of the Lagrangian function ($H = \nabla_{xx}^2 . L$). To attain an optimal point, the parameters must satisfy the Kuhn-Tucker (KT) condition, defined by the Khun-Tucker point as $\nabla_x . L(x^*, \alpha^*) = 0$. The x^* and α^* are the optimum points.

Step 2: This step implicates the calculation of the next iterative point based on the vector d_k, produced as a result of the solution of the QP sub-problem. The first is a merit function $\psi(x)$ is defined as below:

$$\psi(x) = f(x) + \sum_{b=1}^{m} r_b . g_b(x) \tag{8}$$

where r_b is known as the penalty parameter and is initially set to $\frac{\partial f(x)}{\partial g_b(x)}$.

Then, the next x_{k+1} will be determined as:

$$X_{k+1} = X_k + \beta_k . d_k \tag{9}$$

where β_k is the step length parameter and is determined in order to produce a sufficient reduction of the merit function $\psi(x)$.

Step 3: The Hessian approximation H_{k+1} is updated using the Broyden, Flecher, Goldfarb, and Shanno (BFGS)(Kang & Youn, 2019) formula given as follows:

$$H_{k+1} = H_k + \frac{q_k q_k^T}{q_k^T S^k} - \frac{H_k^T H_k}{S_k^T H_k S_k} \tag{10}$$

where $S_k = X_{k+1} - X_k$ and q_k is given by either of the following equations. By using this formula, the Hessian approximate H remains positive definite.

$$q_k = \nabla_x L(X_{k+1}, \beta_k) - \nabla_x L(X_k, \beta_k) \tag{11}$$

$$q_k = \Delta f(X_{k+1}) + \sum_{b=1}^{m} \beta_b . \Delta g_b(X_{k+1}) - [\Delta f(X_k) + \sum_{b=1}^{m} \beta_b . \Delta g_b(X_k)] \tag{12}$$

Step 4: when the s_n becomes a very small value, the program can be stopped. Otherwise, the value of the *k* will be *k = k +1* and the algorithm should start again from step 1 and proceed as described in the steps mentioned above.

2.3. Mathematical modeling of boost converter and BLDC motor

Boost converters are essential components in renewable energy systems, particularly in applications like photovoltaic (PV) systems and wind turbines. They are used to efficiently step up the voltage levels to match the requirements of the load or the grid. The mathematical model of a boost converter typically includes equations describing the relationship between input and output voltages, currents, and the duty cycle of the switching device (such as a MOSFET or IGBT). These models often consider parameters such as inductor and capacitor values, switching frequency, and efficiency.

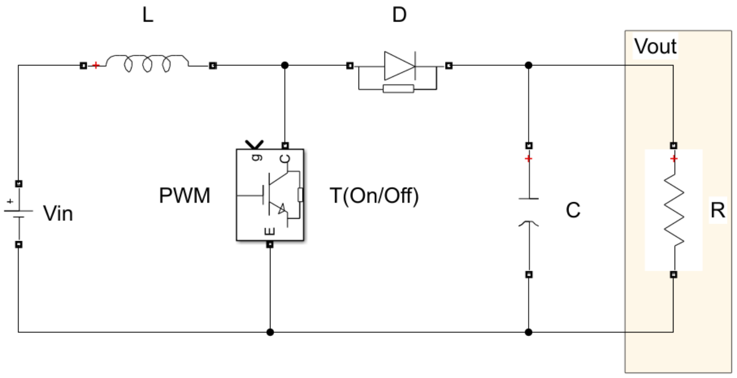

Figure 2 Boost Converter Schematic

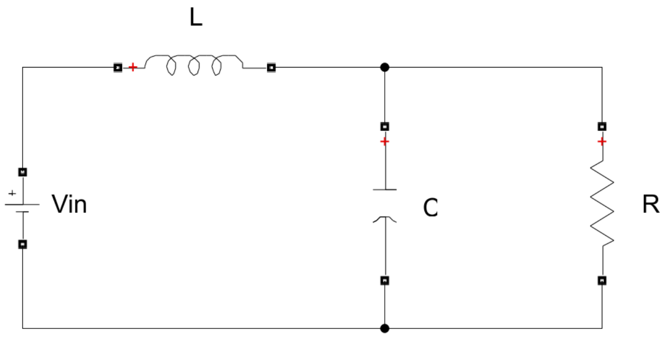

Figure 3 Boost Converter T-On Condition

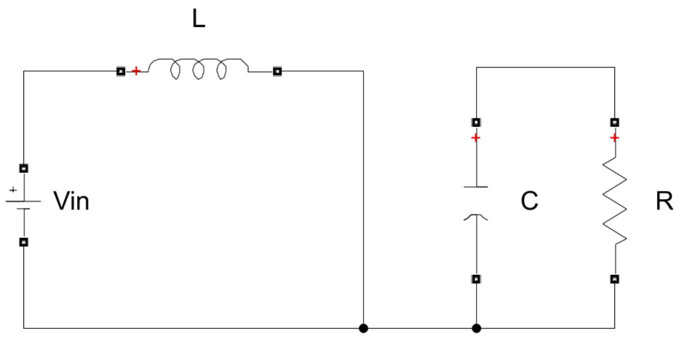

Figure 4 Boost Converter T-Off Condition

The dynamic behavior of the boost converter is crucial for designing effective control strategies, as it directly impacts the system's stability, transient response, and efficiency. Modeling techniques may involve state-space representations, transfer functions, or circuit-based simulations using tools like SPICE. The schematic of the boost converter can be depicted in Figure 2 – 4.

The basic operation of a boost converter can be described by the following equations:

$$V_L = L\frac{\mathrm{d}i_L}{dt} \tag{13}$$

$$i_C = c\frac{\mathrm{d}v_C}{dt} \tag{14}$$

The working process of the DC-DC Boost Converter begins with the switching process, which produces two different things circuits as shown Eq. (13)-(15) below. For the Boost Converter equation in the ON position is defined as:

$$V_L = V_{in}\ x\ PWM \tag{15}$$

Meanwhile for position DC-DC Converter in the OFF is shown:

$$V_L = (V_{in} - V_{out})\ x\ PWM \tag{16}$$

The switching process between two conditions ON and OFF position is determined by the PWM switching frequency and duty cycle as shown:

$$PWM = \frac{(V_{out} - V_{in})}{V_0} f_{pwm}^{-1} \tag{17}$$

The current flowing through the inductor and capacitor are below:

$$i_L = \frac{1}{L} \int V_L dt \tag{18}$$

$$i_C = i_L - i_R \tag{19}$$

The voltage equation on the capacitor is defined:

$$V_C = \frac{1}{C} \int i_C dt \tag{20}$$

The total impedance functions are given by the following Eq. (21)-(25). The DC-DC Boost converter is modeled in the S-domain using the transfer function modeling technique as shown as follow:

$$Z_{total} = Z_1(s) + Z_2(s) \tag{21}$$

$$Z_1(s) = \frac{V_{in}(s)}{I\ (s)} = \left[R\ \frac{1}{C_s}\right] + L_s \tag{22}$$

$$\frac{V_{in}(s)}{I\ (s)} = \frac{RCLs^2 + Ls + R}{RCs + 1} \tag{23}$$

$$I(s) = \frac{RCs + 1}{RCLs^2 + Ls + R} V_{in}(s) \tag{24}$$

$$Z_2(s) = \frac{V_{out}}{I\ (s)} = \frac{R}{RCs + 1} \tag{25}$$

The final equation of the transfer function for the DC-DC Boost converter is produced by Eq. (26). The final equation is defined as:

$$\frac{V_{out}}{V_{in}} = \frac{R}{RCLs^2 + Ls + R} \tag{26}$$

These equations describe the relationship between input and output voltages, output current, inductor current, and the Pulse Width Modulation (PWM) of the boost converter. Here, V_{in} is the input voltage, V_{out} is the output voltage, Rload is the load resistance, and L is the inductance of the boost converter's inductor. The parameters of the boost converter used in this system are shown in Table 2 (Anshory et al., 2024).

Table 2. DC-DC converter parameters

Parameter	Symbol	Value
Resistance	L	100 Ω
Inductance	R	470.000 mH
Capacitance	C	470 μF

BLDC motors are widely used in various applications due to their high efficiency, reliability, and controllability. In the context of renewable energy systems, BLDC motors are commonly employed in applications like electric vehicles, wind turbines, and micro-hydro generators. The mathematical model of a BLDC motor typically comprises equations describing the electromagnetic dynamics, mechanical dynamics, and electrical characteristics. The electromagnetic dynamics of a BLDC motor involve the relationships between the rotor position, electromagnetic torque, and currents flowing through the motor windings. These dynamics are often described using equations derived from the principles of electromagnetism and motor construction. Additionally, the mechanical dynamics of the BLDC motor include equations governing the rotational motion, such as the relationship between torque, speed, and inertia. These equations account for factors like friction, load torque, and mechanical losses.

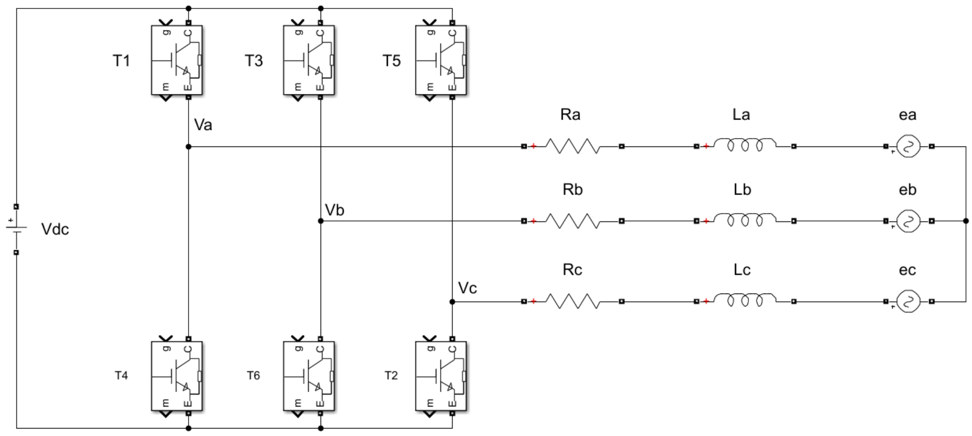

Figure 5 BLDC Schematic Model

The electrical characteristics of the BLDC motor encompass equations defining the voltage-current relationship, back electromotive force (EMF), and resistance of the motor windings. These equations are crucial for understanding how the motor responds to control signals and external loads. The BLDC motor's equivalent circuit is shown in Figure 5. By accurately modeling both the boost converter and the BLDC motor, researchers can analyze the interactions between these components and design optimal control strategies to achieve desired performance metrics such as efficiency, transient response, and stability. Moreover, such models serve as valuable tools for simulation-based studies and experimental validation, facilitating the development and deployment of renewable energy systems.

The mathematical model of a BLDC motor typically includes equations governing its electromagnetic, mechanical, and electrical dynamics by Eq. (27) – (29):

$$V_a = I_a R_a + L_a \frac{di_a}{dt} + e_a \tag{27}$$

$$V_b = I_b R_b + L_b \frac{di_b}{dt} + e_b \tag{28}$$

$$V_c = I_c R_c + L_c \frac{di_c}{dt} + e_c \tag{29}$$

The mechanical time constant for the mathematical equation is defined as:

$$\tau_m = \frac{RJ}{K_e K_t} \tag{30}$$

Where the electrical time constant is shown:

$$\tau_e = \frac{L}{3R} \tag{31}$$

$$K_E = \frac{3RJ}{K_T \tau_m} \tag{32}$$

For BLDC motor equation is defined as:

$$G(s) = \frac{\omega_m}{V_s} = \frac{1/K_e}{\tau_m \tau_e S^2 + \tau_m s + 1} \tag{33}$$

where K_t is the torque constant, $I_a, I_b, and\ I_c$ are the armature current per phase, $e_a, e_b, and\ e_c$ are return EMF per phase, K_e is the back EMF constant, ω_m is the rotor angular velocity, V_s is a voltage source, J is the rotor's moment of inertia, $R = R_a = R_b = R_c$ is armature resistance, $L = L_a = L_b = L_c$ is the armature self-inductance, τ_m is mechanical torque, τ_e is the electrical torque. These equations describe the relationship between electromagnetic torque, back EMF, rotor angular velocity, and mechanical dynamics. They are essential for understanding the motor's behavior under different operating conditions and for designing control strategies to achieve desired performance objectives. The nominal voltage of the BLDC motor is 24 volts with 8 poles. The BLDC motor parameters are shown in Table 3 (Anshory et al., 2024).

Table 3. BLDC Motor parameters

Parameter	Symbol	Value
Torque Constant	Kt	0.0521 $N\,m/A$
Back EMF constant	Ke	0.0521 $V/rad/s$
Rotor Inertia Moment	J	$19.10^{-6}\ kg.m^2$
Armature Resistance	R	1.835 Ω
Armature Inductance	L	0.287 mH

2.4. PID Controller

A controller known as the Proportional Integral Derivative (PID) controller leverages the feedback characteristics of a system to evaluate the accuracy of an instrumentation system. The PID controller is also used to enhance the dynamic response and reduce steady-state errors. The proportional part of PID works to correct in magnitude change depending on the error size, hence ensuring that there is a fast decrease of the error and providing an initial reaction of the system, therefore the integral component of the controller works to minimize steady-state errors, while the derivative component enhances the transient response (Bharat et al., 2019; Bistak et al., 2023; Shah and Agashe, 2016). It has three different components: proportional, integral, and derivative. These components can be used individually or simultaneously in any combination depending on the type of plant process or the response required (Ibrahim et al., 2019; Prommee and Angkeaw, 2018; Shah and Agashe, 2016). The transfer function of the PID controller is mathematically represented by the equations provided in Eq. (34) and (35).

$$k_p + \frac{k_i}{s} + k_d s = \frac{k_d s^2 + k_p s + k_i}{s} \tag{34}$$

$$k_p e + k_i \int e dt + k_d \frac{de}{dt} \tag{35}$$

To minimize the error value in the PID tuning process, several equations are used as error comparison functions These include Integral Absolute Error (IAE), Integral Square Error (ISE), Integral Time-weighted Square Error (ITSE), and Integral Time-weighted Absolute Error (ITAE) ITAE is utilized in this system because it provides better performance in delivering smoother and faster responses, while also suppressing errors within the system response time. In this case, it can be said that ITAE is the objective function of optimization carried out to obtain the values of k_p, k_i, and k_d in the PID tuning process. ITAE equation is defined as:

$$ITAE = \int_{t=0}^{Ts} t.|e(t)|dt \tag{36}$$

$e(t)$ is the error value at t time, $V(t)$ is the output of BLDC voltage, $r(t)$ is the set point of the photovoltaic, Ts is the simulation time. The whole system block diagram controlled by PID is shown in Figure 6 and the Simulink simulation for optimization is depicted in Figure 7.

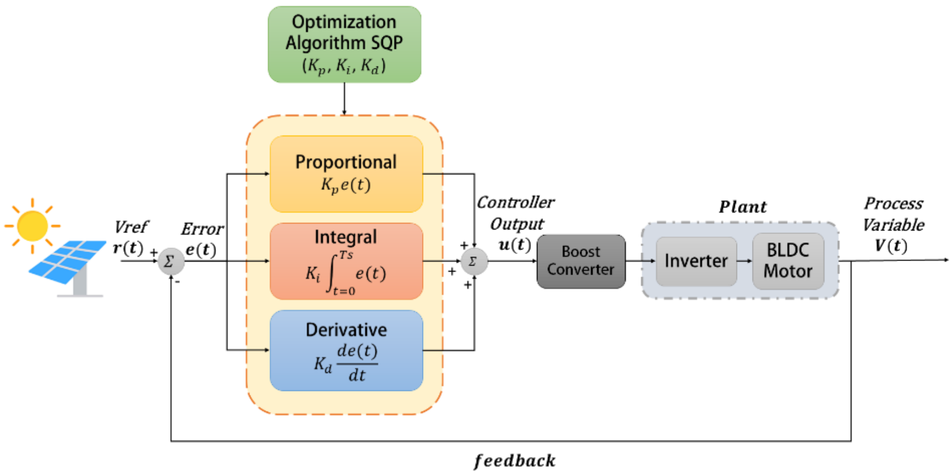

Figure 6 System block diagram

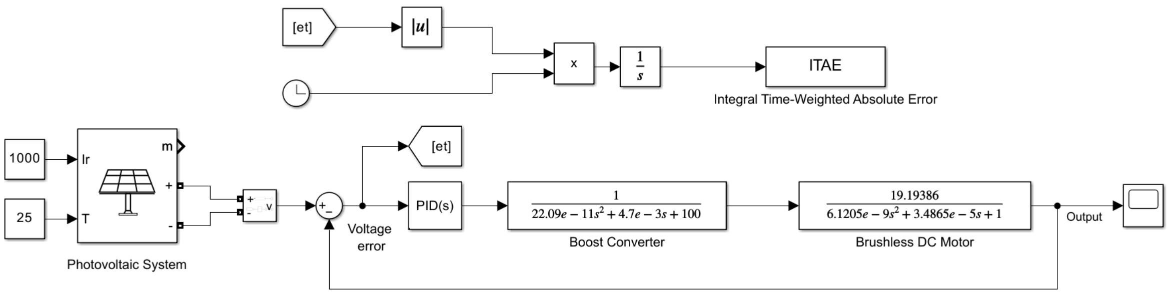

Figure 7 Block Diagram for SQP-PID Optimization in Simulink

3. Results and Discussion

The discussion of this study aims to compare the optimization of the use of several PID models, both conventional and those that have been developed. Based on several previous studies found, several models were implemented in this study, namely conventional PID, GMO – PID, Firefly algorithm, and SQP – PID. The SQP – PID model proposed by this study is a PID controller optimization technique for using a BLDC motor booster converter by considering PV as renewable energy. To support the simulation process, the electrical characteristics obtained from using PV parameters are modeled. This is the initial stage of the simulation process, so that the obtained data can be used as input material for the simulation process in various optimization models. The electrical characteristics used in this study are the I – V and P – V characteristic graphs. This model provides information related to the operational conditions of the system. The graphic characteristics of the PV module are shown in Figure 3. In the simulation and testing, the 200 W Solar Photovoltaic has been modeled based on its electrical characteristics. These characteristics are important indicators for recognizing the efficiency of the PV system in producing electricity obtained from sunlight.

Optimization of the PID controller on the DC-DC Boost Converter aims to improve overall system performance and efficiency. By tuning PID controller parameters, the system can achieve better response characteristics, including faster transient response, reduced settling time, and minimized overshoot or oscillation, ensuring efficient output voltage regulation under a wide range of load and input conditions. Stability, in this system, refers to the ability of the generated voltage to reach and maintain an equilibrium state following a disturbance. The disturbance could refer to the uncertainty of photovoltaic. Regardless, Instability is characterized by the presence of irregular oscillations and divergence. Steady state, conversely, is achieved when the voltage has stabilized at a constant value, exhibiting no further fluctuations. Optimization helps mitigate stability issues, improving stability for reliable operation, especially in renewable energy applications where input source fluctuations are common. Optimized PID controller tuning contributes to increased energy efficiency by minimizing losses and maximizing power conversion efficiency, which is critical for sustainable operation.

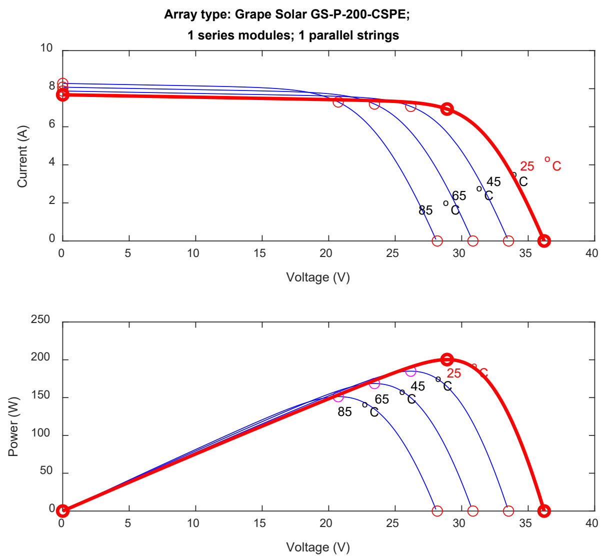

Figure 8 Graphic I–V and P–V characteristics of the PV module

This optimization also allows the controller to adapt to changing conditions, maintaining optimal performance across a wide range of operating conditions, thereby increasing system reliability and robustness while reducing control effort and increasing component longevity. In the optimization process, the simulation block diagram relies on the Simulink feature as shown in Figure 8. This process aims to obtain proportional values. The comparison results between SQP – PID and conventional PID simulation are shown in Figure 9. The graph of the simulation results using SQP – PID shows that the rise time obtained by this method is 344 s, while the conventional method has a higher value of 649 s. This shows that the SQP – PID model has a faster initial response compared to the conventional model. The overshoot performance shown by the SQP – PID model is also better, namely zero percent compared to the conventional model of 11.1%. Additionally, the reduction in completion time between the two is quite significant. The SQP – PID model can be completed in 480 s, while the conventional model takes 721 s. By looking at the results it can be seen that the stability of the SQP – PID model is also better than the conventional model without any excessive deviation.

Besides the SQP – PID model, other models are also proposed in this study. This aims to obtain the best optimization model among the models used in this study. The next model is the GMO – PID model as shown in Figure 9. The simulation results graph shows that the

GMO – PID model is almost the same as the SQP – PID model when compared with the conventional model. The GMO–PID model has better stability than the conventional model. GMO – PID overshoot performance has a value of zero percent, with a completion time of 529 s. Meanwhile, the rise time value for GMO – PID is 379 s. As another comparison, the FA – PID model is analyzed in this study. Figure 9 also shows a comparison between the FA – PID model and conventional PID. In this case, the simulation results graph shows that FA – PID has a slower initial response than the conventional model. The FA – PID settling time value in this study is 1108 s. However, the overshoot performance of the FA – PID model decreases significantly to zero with better stability than conventional PID. In previous research conducted by (Anshory et al., 2024) A similar trend is also shown in FA–PID compared with conventional PID. Next, all optimization models are compared in one graph of test results as shown in Figure 9. Based on the test results, the SQP – PID model has a better overall value compared to the GMO – PID and FA – PID optimization models. However, when compared with conventional models, all optimization models are still better than conventional models in terms of stability.

The SQP – PID and GMO – PID models almost give the same value, but not quite significantly. The difference in values in the model can be seen in the settling time and rise time obtained. SQP – PID has a settling time value of 480 s with a rise time of 344 s, while GMO – PID has a settling time value of 529 s with a rise time of 379 s. SQP – PID can achieve stability more quickly with a better initial response compared to the GMO – PID model.

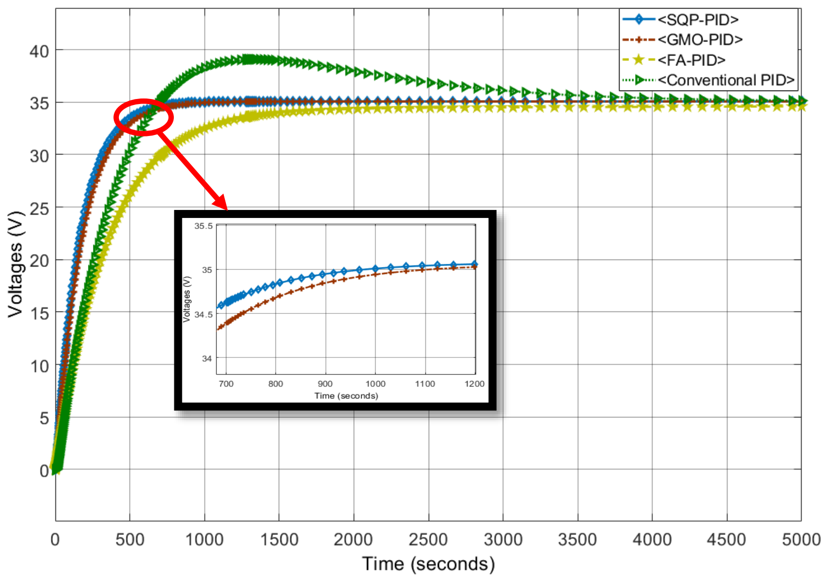

Figure 7 PID Tunning Optimization Comparison Results

The performance parameter comparisons resulting from various PID tuning methods, including conventional PID, derivative-based optimization, and metaheuristic-based optimization, are presented in Table 4. The proposed method exhibits a better ITAE value compared to both metaheuristic and conventional PID. The ITAE achieved is 7.18% smaller than that of FA and 9.64% smaller than GMO. In addition to the smaller error performance, the time required by the proposed method significantly decreases, being up to 92.45% faster than GMO and 93.91% faster than FA. The simulation time comparison for conventional PID cannot be defined, as it utilizes a trial-and-error approach, which is typically more time-consuming compared to optimization methods, with substantially larger errors.

Table 4 Comparison of Various Tuning Methods

Performance Parameters	Conventional PID	**Proposed Method SQQ-PID**	FA-PID (Anshory et al., 2024)	GMO-PID
ITAE	14892679.42	**1018555.64**	1097300	1127200.65
ISE	207641.55	**104823.75**	227060	114767.93
ITSE	55107347.94	**8409668.50**	4522800	10136380.24
IAE	15841.89	**5816.98**	14922	6364.59
Simulation Time (s)	-	**55.71**	914.49	737.75
Kp	101.44	**210**	97.76	191.38
Ki	0.08	**0.03**	0.01	0.02
Kd	-292.72	**0.19**	-0.13	-4.86
Rise Time (s)	649.81	**344.66**	756.68	379.30
Peak Amplitude	39.08	**35.08**	34.25	35.07
Settling Time (s)	721.73	**480.33**	1108	529.18
Overshoot (%)	11.1	**0**	0	0

4. Conclusions

Based on the results of tests that have been carried out on boost converter planning in all models as a BLDC motor driver using a PID controller, the SQP - PID model as a whole obtained the most superior value compared to other optimization models and conventional PID. This shows that the performance of BLDC motors with conventional PID controller can be improved by implementing PID controller optimization. All optimization methods can reduce the achievement time compared with conventional PID, especially the proposed SQP – PID model. In this case, the system reaction can increase as measured by the increase in system speed in achieving work stability. The SQP – PID method shows improved performance by reducing completion time by 33.42% compared to conventional PID. Finally, in terms of overshoot performance, the SQP – PID method decreased significantly from 11.1% to 0%. Not only did the SQP – PID optimization method decrease, but all optimization methods also decreased to 0%. This indicates that the system is more reliable after optimization methods have been carried out to achieve ideal conditions.

Acknowledgments

The Author thanks for the research funding within contract number 194.2/UN27.22/PT.01.03/2024.

Conflict of Interest

The authors declare no conflicts of interest.

References

Aguila-Leon, J., Vargas-Salgado, C., Hurtado-Perez, E., Garcia, E.X.M., Chiñas-Palacios, C., 2021. Particle Swarm Optimization, Genetic Algorithm and Grey Wolf Optimizer Algorithms Performance Comparative for a DC-DC Boost Converter PID Controller. Advances in Science, Technology and Engineering Systems Journal, Volume 6(1), pp. 619–625.

Aiman Setiawan, E.A.S., 2017. Optimization of a Photovoltaic Power Plant in Indonesia with Proper Tilt Angle and Photovoltaic Type using a System Advisor Model. International Journal of Technology, Volume 8(3), pp. 291–319.

Ajiwiguna, T.A., Kirom, M.R., 2024. Uninterrupted Electricity Supply using Off-Grid Solar PV

Systems for Remote Areas. International Journal of Technology, Volume 15(5), pp. 291–319.

Ali, H.F.J.A., AlKassem, A., Abdullah, M.P., 2024. Optimal Design and Performance Analysis of Multiple Photovoltaic with Grid-Connected Commercial Load. International Journal of Technology, Volume 15(4), pp. 291–319.

Alshareef, A., Shah, R., Mithulananthan, N., Alzahrani, S., 2021. A New Global Index for Short Term Voltage Stability Assessment. IEEE Access, Volume 9, pp. 36114–36124.

Anshory, I., Jamaaluddin, J., Wisaksono, A., Sulistiyowati, I., Hindarto, Rintyarna, B.S., Fudholi, A., Rahman, Y.A., Sopian, K., 2024. Optimization DC-DC boost converter of BLDC motor drive by solar panel using PID and firefly algorithm. Results in Engineering, Volume 21, pp. 101727.

Aseem, K., Selva Kumar, S., 2020. Closed loop control of dc-dc converters using pid and fopid controllers. International Journal of Power Electronics and Drive Systems, Volume 11(3), pp. 1323–1332.

Ben Safia, Z., Kharrat, M., Allouche, M., Mohamed, C., 2021. TS Fuzzy Fault-Tolerant Tracking Control of a PV Pumping System Based on an Induction Motor. IETE Journal of Research, Volume 7, pp. 4826–4835.

Bharat, S., Ganguly, Arunangshu, Chatterjee, R., Basak, B., Sheet, D.K., Ganguly, Anirban, 2019. A Review on Tuning Methods for PID Controller. Asian Journal For Convergence In Technology (AJCT) ISSN -2350-1146, Volume 0(0 SE-Article).

Bistak, P., Huba, M., Vrancic, D., Chamraz, S., 2023. IPDT Model-Based Ziegler–Nichols Tuning Generalized to Controllers with Higher-Order Derivatives. Sensors, Volume 23(8).

Bueso, M.C., Paredes-Parra, J.M., Mateo-Aroca, A., Molina-García, A., 2022. Sensitive Parameter Analysis for Solar Irradiance Short-Term Forecasting: Application to LoRa-Based Monitoring Technology. Sensors, Volume 22(4).

De, S., Swathika, O.V.G., Tewari, N., Venkatesan, A.K., Subramaniam, U., Bhaskar, M.S., Padmanaban, S., Leonowicz, Z., Mitolo, M., 2020. Implementation of Designed PV Integrated Controlled Converter System. IEEE Access, Volume 8, pp. 100905–100915.

Delfianti, R., Rovianto, E., Budi, A.L.S., Priyadi, A., Abadi, I., Soeprijanto, A., 2022. Evaluation of the Energy Transaction Cost for Microgrid-Based Wheeling System Using Power Flow Tracing: a Case Study. International Review of Electrical Engineering, Volume 17(2), pp. 154–163.

Devaraj, S. V, Gunasekaran, M., Sundaram, E., Venugopal, M., Chenniappan, S., Almakhles, D.J., Subramaniam, U., Bhaskar, M.S., 2021. Robust Queen Bee Assisted Genetic Algorithm (QBGA) Optimized Fractional Order PID (FOPID) Controller for Not Necessarily Minimum Phase Power Converters. IEEE Access, Volume 9, pp. 93331–93337.

Eleftheratos, K., Raptis, I.-P., Kouklaki, D., Kazadzis, S., Founda, D., Psiloglou, B., Kosmopoulos, P., Fountoulakis, I., Benetatos, C., Gierens, K., Kazantzidis, A., Richter, A., Zerefos, C., 2024. Atmospheric parameters affecting spectral solar irradiance and solar energy (ASPIRE). AIP Conference Proceedings, Volume 2988(1), pp. 110002.

Gao, Y., 2023. PID-based search algorithm: A novel metaheuristic algorithm based on PID algorithm. Expert Systems with Applications, Volume 232, pp. 120886.

Ghamari, S.M., Narm, H.G., Mollaee, H., 2022. Fractional-order fuzzy PID controller design on buck converter with antlion optimization algorithm. IET Control Theory & Applications, Volume 16(3), pp. 340–352.

Grigoraş, G., Neagu, B.-C., Ivanov, O., Livadariu, B., Scarlatache, F., 2022. A New SQP Methodology for Coordinated Transformer Tap Control Optimization in Electric

Networks Integrating Wind Farms. Applied Sciences, Volume 12(3).
Hamid, A.-K., Obaid, W., Ghenai, C., 2021. Hybrid Solar/Wind/Diesel Water Pumping System: A Case Study in Dubai United Arab Emirates. International Journal of Electrical and Computer Engineering, Volume 11(3), pp. 2062–2067.
Hekimoğlu, B., Ekinci, S., 2020. Optimally Designed PID Controller for a DC-DC Buck Converter via a Hybrid Whale Optimization Algorithm with Simulated Annealing. Electrica, Volume 20(1), pp. 19–27.
Ibrahim, M., Mahmood, A., Sultan, N., 2019. Optimal PID controller of a brushless dc motor using genetic algorithm. International Journal of Power Electronics and Drive Systems (IJPEDS), Volume 10(2), pp. 822.
Izci, D., Hekimoğlu, B., Ekinci, S., 2022. A new artificial ecosystem-based optimization integrated with Nelder-Mead method for PID controller design of buck converter. Alexandria Engineering Journal, Volume 61(3), pp. 2030–2044.
Janprom, K., Permpoonsinsup, W., Wangnipparnto, S., 2020. Intelligent Tuning of PID Using Metaheuristic Optimization for Temperature and Relative Humidity Control of Comfortable Rooms. Journal of Control Science and Engineering, Volume 2020(1), pp. 2596549.
Jia, Y., Alva, G., Fang, G., 2019. Development and applications of photovoltaic–thermal systems: A review. Renewable and Sustainable Energy Reviews, Volume 102(March 2019), pp. 249–265.
Joseph, S.B., Dada, E.G., Abidemi, A., Oyewola, D.O., Khammas, B.M., 2022. Metaheuristic algorithms for PID controller parameters tuning: review, approaches and open problems. Heliyon, Volume 8(5), pp. e09399.
Khleaf, H., Nahar, A., Subhi, A., 2019. Intelligent control of DC-DC converter based on PID-neural network. International Journal of Power Electronics and Drive Systems (IJPEDS), Volume 10(4), pp. 2254.
Khodabakhshian, A., Pour, M.E., Hooshmand, R., 2012. Design of a robust load frequency control using sequential quadratic programming technique. International Journal of Electrical Power & Energy Systems, Volume 40(1), pp. 1–8.
Kumar, P.P., Vinaykumar, M., 2023. A Review On The Estimate Solar PV Cell Variables For Efficient Photovoltaic Systems. International Journal of Smart grid, Volume 7(V7i3).
Liu, Ye, Qian, Y., Feng, S., Berg, L.K., Juliano, T.W., Jiménez, P.A., Grimit, E., Liu, Ying, 2022. Calibration of cloud and aerosol related parameters for solar irradiance forecasts in WRF-solar. Solar Energy, Volume 241(15 July 2022), pp. 1–12.
Luo, X., Lv, J.-H., Sun, G., 2022. Continuation methods with the trusty time-stepping scheme for linearly constrained optimization with noisy data. Optimization and Engineering, Volume 23(1), pp. 329–360.
Malla, S.G., Malla, P., Malla, J.M.R., Singla, R., Choudekar, P., Koilada, R., Sahu, M.K., 2022. Whale Optimization Algorithm for PV Based Water Pumping System Driven by BLDC Motor Using Sliding Mode Controller. IEEE Journal of Emerging and Selected Topics in Power Electronics, Volume 10(4), pp. 4832–4844.
Mao, T., Zhang, X., Zhou, B., 2019. Intelligent Energy Management Algorithms for EV-charging Scheduling with Consideration of Multiple EV Charging Modes. Energies, Volume 12(2), pp. 265.
MathWorks, 2004. MATLAB R2024b. Natick, MA. The MathWorks, Inc.
Miqoi, S., El Ougli, A., Tidhaf, B., 2019. Adaptive fuzzy sliding mode based MPPT controller for a photovoltaic water pumping system. International Journal of Power Electronics and Drive Systems (IJPEDS), Volume 10(1), pp. 414.
Mitra, L., Rout, U., 2022. Optimal control of a high gain DC- DC converter. International

Journal of Power Electronics and Drive Systems (IJPEDS), Volume 13(1), pp. 256.

Mohammed, H., Farah, N., 2019. Photovoltaic (PV) System Applied To Induction Motor Drives. International Journal of Advanced Science and Technology, Volume 28(1), pp. 363–373.

Mohasseb, S., Moradi, M., Sokhansefat, T., kowsari, F., Kasaeian, A., Mahian, O., 2017. A novel approach to solve inverse heat conduction problems: Coupling scaled boundary finite element method to a hybrid optimization algorithm. Engineering Analysis with Boundary Elements, Volume 84, pp. 206–212.

Munisekhar, S., Marutheeswar, G., Sujatha, P., Vadivelu, K.R., 2020. A novel approach for the fastest MPPT tracking algorithm for a PV array fed BLDC motor driven air conditioning system. Indonesian Journal of Electrical Engineering and Computer Science, Volume 18(2), pp. 622.

Nasruddin, Sinambela, H., 2015. Design and Experimental Study of Air Conditioning System using Brushless Direct Current (BLDC) Compressor in National Electric Car. International Journal of Technology, Volume 6(6), pp. 291–319.

Osman, N., Khalid, H.M., Sweidan, T.O., Abuashour, M.I., Muyeen, S.M., 2022. A PV powered DC shunt motor: Study of dynamic analysis using maximum power Point-Based fuzzy logic controller. Energy Conversion and Management: X, Volume 15, pp. 100253.

Osorio, E., Becerra, G., Palafox-Roca, A., Ledesma-Alonso, R., 2019. An Empiric-Stochastic Approach, Based on Normalization Parameters, to Simulate Solar Irradiance. Journal of Solar Energy Engineering, Volume 141(4), pp. 1.

Prommee, P., Angkeaw, K., 2018. High performance electronically tunable log-domain current-mode PID controller. Microelectronics Journal, Volume 72, pp. 126–137.

Saaid, F.I., Tseung-Yuen Tseng, Winie, T., 2018. PVdF-HFP Quasi-solid-state Electrolyte for Application in Dye-sensitized Solar Cells. International Journal of Technology, Volume 9(6), pp. 291–319.

Setyawati, R.N.H.O., Taufik, T., Sawitri, D.R., Suyono, H., Yuniar, F., 2024. A Modified Perturb-and-Observe Control for Improved Maximum Power Point Tracking Performance on Grid-Connected Photovoltaic System. International Journal of Technology, Volume 15(1), pp. 291–319.

Shah, P., Agashe, S., 2016. Review of fractional PID controller. Mechatronics, Volume 38, pp. 29–41.

Sugiantoro, N., Wibowo, R., Lystianingrum, V., Rovianto, E., Triwijaya, S., 2021. Optimal Power Flow With Dynamic Line Rating Using Quadratically Constrained Quadratic Program Method, in: 1st International Conference on Electronic and Electrical Engineering and Intelligent System (ICE3IS),. pp. 54–59.

Wibowo, R.S., Rovianto, E., Lystianingrum, V., Aryani, N.K., Penangsang, O., 2023. Dynamic Optimal Power Flow for Microgrids Considering Efficiency and Lifetime of Battery Using MINLP. International Review of Electrical Engineering, Volume 18(1), pp. 15–24.